Electron Transfer Dynamics in Dye Sensitized Nanocrystalline Solar Cells Using a Polymer Electrolyte

ARTICLE *in* THE JOURNAL OF PHYSICAL CHEMISTRY B · JULY 2001

Impact Factor: 3.3 · DOI: 10.1021/jp010420q

Electron Transfer Dynamics in Dye Sensitized Nanocrystalline Solar Cells Using a Polymer Electrolyte

Ana F. Nogueira and Marco-A. De Paoli*

Laboratório de Polímeros Condutores e Reciclagem, Instituto de Química, UNICAMP, C. Postal 6154, 13083-970 Campinas SP, Brazil

Ivan Montanari,[†] Richard Monkhouse,[†] Jenny Nelson,[‡] and James. R. Durrant*,[†]

Centre for Electronic Materials and Devices, Departments of Chemistry and Physics, Imperial College, London SW7 2AY, United Kingdom

Received: February 2, 2001; In Final Form: May 13, 2001

Transient absorption spectroscopy was employed to study electron-transfer dynamics in dye sensitized nanocrystalline solar cells incorporating a polymer electrolyte, poly(epichlorohydrin-*co*-ethylene oxide) containing NaI and I_2. Solar cells employing this solid-state electrolyte have yielded solar to electrical energy conversion efficiencies of up to 2.6%. Electron-transfer kinetics were collected as a function of electrolyte composition, white light illumination, and device voltage and correlated with current/voltage characterization of the cell. The yield of electron injection from the dye excited state into the TiO_2 electrode was found to be insensitive to electrolyte composition or cell operating conditions. Regeneration of the dye ground state by electron transfer from I^- ions in the polymer electrolyte exhibited half times of 4−200 μs, depending upon the concentration of NaI in the polymer electrolyte. A long-lived product of the regeneration reaction was observed and assigned to the I_2^- radical. At low NaI concentrations, kinetic competition was observed between this regeneration reaction and charge recombination of the oxidized dye with electrons injected into the semiconductor. The decay kinetics of the dye cation, and the yield of I_2^-, were found to be unchanged by illumination of the cell under either short circuit or open circuit (V_{oc} = 0.75 V) conditions. From these observations, we conclude that the charge recombination dynamics in this cell are not strongly dependent upon the TiO_2 Fermi level over this voltage range. Analogy with studies of recombination dynamics in three electrode photoelectrochemical cells employing a redox inactive liquid electrolyte suggest this observation may be related to the Lewis base nature of the polymer employed.

Introduction

Photoelectrochemical cells based on sensitization of nanocrystalline TiO_2 by molecular dyes have attracted great attention since their first announcement as efficient photovoltaic devices.[1] Nanocrystalline TiO_2 films sensitized with cis-[$(dcbH_2)_2Ru(SCN)_2$] (where $dcbH_2$ = 4,4′-$(CO_2H)_2$-2,2′-bipyridine) dye (D), have yielded solar energy into electricity conversion efficiencies of up to 10%.[2] The function of such devices is based on the injection of an electron from a photoexcited state of the sensitizer dye (D*) into the conduction band of the nanocrystalline semiconductor, as illustrated in Figure 1. These cells typically employ a liquid electrolyte (usually an iodide/triiodide redox active couple dissolved in acetonitrile) to rereduce the dye cation (D^+). Regeneration of iodide ions, which are oxidized in this reaction to triiodide, is achieved at a platinised counter electrode.

The charge separation in a nanocrystalline semiconductor is thought not to depend on a built-in electrical field, i.e., a Shottky barrier, but is mainly determined by electron kinetics at the semiconductor/dye/electrolyte interface (SEI)[3], as detailed in Figure 1. The rate of electron injection, k_{inj}, must be higher than the decay rate of the dye excited state to ground. In addition, the rate of recombination of the dye cations with electrons injected into the semiconductor, k_{cr1}, must be lower than the rate of rereduction of the dye cation by iodide, k_{rr}. For liquid electrolyte cells, the electron injection process occurs on femtosecond-picosecond time scales for a range of different sensitizer dyes with a high quantum yield.[4−7] The corresponding charge recombination reaction between injected electrons and dye cations (k_{cr1}), exhibits time constants ranging from picoseconds to milliseconds and is very sensitive to electrolyte composition and external applied bias.[8−10] Finally, charge transport of electrons through the TiO_2 electrode and triiodide through the electrolyte must be sufficiently fast to avoid recombination of these species, labeled as k_{cr2} in Figure 1. This latter recombination mechanism is responsible for the dark current observed for these solar cells under bias in the dark.

The use of a liquid electrolyte in dye sensitized photoelectrochemical devices compromises their long-term durability and stability due to, for example, evaporation or leakage of the solvent and contamination with water or impurities. Such stability issues are important for the commercialization of this technology. To address this problem, attention is increasingly focusing on developing solid state or "quasi solid state" replacements for this liquid electrolyte. Organic and inorganic hole conductors,[11−15] polymer gel electrolytes,[16,17] and the addition of polymeric gelling agents in the liquid electrolyte to

* To whom correspondence should be adressed. E-mail: j.durrant@ic.ac.uk, mdepaoli@iqm.unicamp.br.
[†] Department of Chemistry, Imperial College, London.
[‡] Department of Physics, Imperial College, London.

10.1021/jp010420q CCC: $20.00
Published on Web 07/18/2001

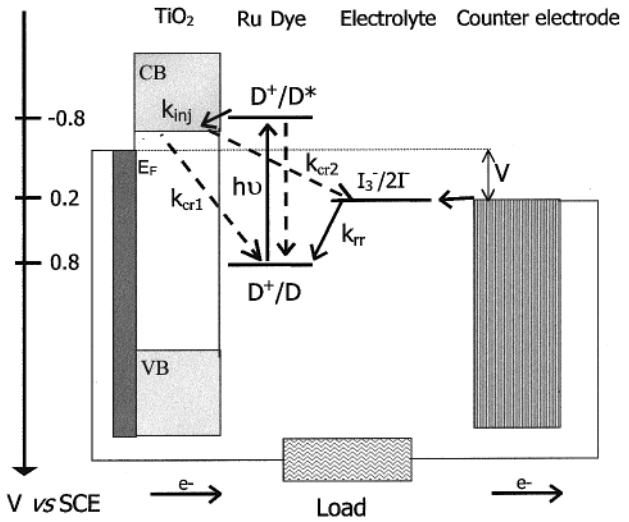

Figure 1. Schematic description of a TiO_2 dye sensitized photoelectrochemical cell, exhibiting the main processes. Optical excitation of the dye gives rise to an ultrafast electron injection into TiO_2 conduction band states (k_{inj}). The oxidized dye cation is then, rereduced by I^-/I_3^- redox couple present in the electrolyte (k_{rr}). This process must be faster than back electron transfer from electrons photoinjected into the TiO_2 conduction band to dye cation (k_{cr1}). Also indicated is the recombination reaction k_{cr2} between injected electrons and oxidized redox species in the electrolyte (I_3^- ions), corresponding to dark current losses within the cell.

promote its solidification[18,19] are all being investigated for this purpose. Recently, we reported the use of an elastomer, poly(epichlorohydrin-*co*-ethylene oxide) (Epichlomer-16), filled with NaI and I_2 as polymer electrolyte for these kind of cells. We found this polymer electrolyte achieved good penetration throughout the film pores.[17] Devices employing this electrolyte exhibit an overall solar to electrical conversion efficiency of 2.6% when irradiated at moderate light levels (10 mW cm^{-2}) and monochromatic incident photon to current efficiencies of up to 61%.[20]

Studies of devices employing liquid electrolytes have demonstrated that modulation of electrolyte composition influences not only those functions directly associated with their properties (e.g., dye cation rereduction, k_{rr} and transport kinetics) but also the properties of the TiO_2 electrode (e.g., electron injection and recombination kinetics, k_{inj} and k_{cr1}).[4,8−9] Studies of the function of solid-state dye sensitized photoelectrochemical cells have been limited to date.[15] The nature, transport mechanism, and ionic conductivity of the polymer electrolyte employed may influence all of the electron transfer and transport properties illustrated in Figure 1, thereby controlling device function. Studies of these properties are essential for further optimization of these types of cell.

In this work, we employed nanosecond-millisecond transient absorption spectroscopy to evaluate the electron-transfer dynamics in dye sensitized nanocrystalline solar cells using a polymer electrolyte and relate these kinetic studies to solar cell function.

Materials and Methods

Sample Preparation. Transparent nanocrystalline TiO_2 films were prepared as detailed by Topoglidis et al.[22] The methodology essentially followed that of Barbe et al,[23] and employed the deposition by doctor blading of a 12% aqueous solution of ~15 nm TiO_2 colloids onto conducting glass substrate (F-doped SnO_2 TEC15, sheet resistance ~15 Ω/sq), followed by firing at 450 °C for 30 min in an airgun. The resultant 4 μm thick TiO_2 films were sensitized with the dye *cis*-bis(isothiocyanato)-bis(2,2′-bipyridyl-4,4′-dicarboxylato)-ruthenium(II) bis tetrabutylammonium ($Ru(dcbpy)_2(NCS)_2$) (Johnson & Matthey Ltd.), by immersing overnight in a 1.2×10^{-3} mol L^{-1} acetonitrile/*tert*-butyl alcohol 1:1 solution. Afterward, the electrode was washed with the solvent mixture and dried in a moisture free atmosphere. The optical density of the films was typically of 0.2−0.3 at 600 nm and ~1.0 at 540 nm (sample absorption maximum).

The polymer electrolyte film was prepared by casting of a solution of poly(epichlorohydrin-*co*-ethylene oxide), Epichlomer-16 (Daiso Co. Ltd., Osaka, Japan), containing 0.3 g of the elastomer dissolved in 25 mL of acetone, followed by the addition of 0.03 g of NaI. This salt content gives rise to a concentration of 9% NaI (w/w), corresponding to the maximum of ionic conductivity of the system (1.5×10^{-5} S cm^{-1}, 30 °C and $[H_2O] < 1$ ppm).[24] For experiments as a function of I^- concentration, 1 to 20% NaI (w/w) was added to the solution, with the appropriate co-addition of $NaClO_4$ to maintain a constant Na^+ concentration. Thus, the changes observed can be related to different I^- concentrations alone. Samples containing a nonactive redox electrolyte were also prepared for comparison, employing 9% $NaClO_4$ (w/w) in Epichlomer-16. Polymer solutions (~400 μL) were dropped over the modified electrode and allowed to dry for 1 h. Afterward, a thin glass cover slide was placed over the electrolyte film. All the samples were stored under dry conditions and in the dark. All the experiments were carried out at room temperature.

To evaluate the transient experiments under bias control and the I−V characteristics, complete solid-state solar cells were assembled using this polymer electrolyte. The addition of 0.003 g of I_2 in the polymer solution previously described was necessary in order to achieve cell function. Thus, a solution of elastomer containing 9 and 0.9% NaI and I_2 (w/w), respectively, was dropped onto a dye-sensitized TiO_2 film (4 μm thick), allowed to dry and then pressed against a platinised counter electrode. The cells were studied unsealed, with their mechanical integrity being maintained by an external clamp.

To prepare the transparent platinum counter electrode, a 0.05 M solution of H_2PtCl_6 in 2-propanol was deposited onto the conducting glass and the electrode was fired at 400 °C for 20 min.

Control experiments were performed employing a liquid electrolyte and three- electrode photoelectrochemical cell in order to allow control of potential applied to the TiO_2 in the absence of redox carriers in the electrolyte. The cell employed dye-sensitized TiO_2 films as the working electrode, an Ag/AgCl reference electrode and platinum wire as counter electrode. Transient absorption data was recorded as a function of applied bias for a series of different electrolytes. The three electrolytes employed were propylene carbonate, containing 0.1 M $LiClO_4$, 0.1 M $NaClO_4$, and 0.1 M $NaClO_4$ with additional 0.5 M *tert*-butyl-pyridine.

IV curves were obtained with a home-built IV characterization interface coupled to a computer. For experiments under simulated sunlight, samples were irradiated with a 150 W Xe lamp through an AM 1.5 filter (Bentham Instruments), calibrated by a thermal power meter and externally calibrated GaAs photovoltaic cell. Neutral density filters were used to change the light intensity.

Transient Absorption Spectroscopy. Nanosecond to millisecond transient absorption experiments employed a nitrogen laser pumped dye laser as excitation source. Data were collected employing low intensity, 600 nm excitation pulses (0.3 mJ cm^{-2},

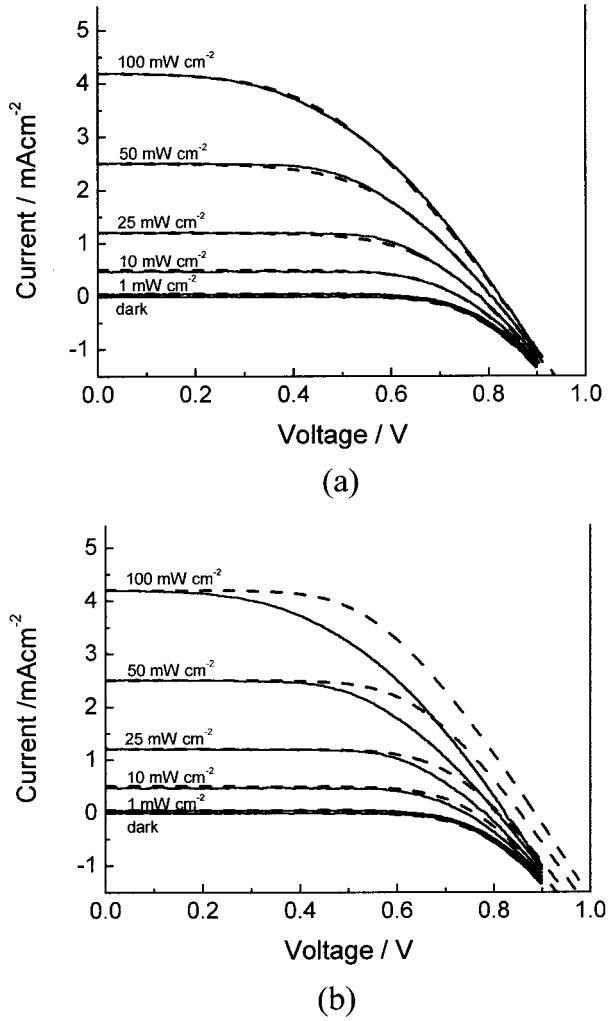

Figure 2. I−V characteristics of the TiO_2/dye nanocrystalline solar cell using the polymer electrolyte at different light intensities. Full lines are experimental data. Dashed lines are fits to the data based (a) on eq 1, and (b) on the simplified form of eq 1 omitting the light dependent recombination term (i.e., $k = 0$).

repetition rate 0.1−0.2 Hz, < 1 ns duration) resulting in approximately one injected electron per colloidal particle. The probe light source was a 150 W tungsten lamp. The monitoring wavelength from the lamp was selected by using a monochromator, typically set to monitor the transient signal at 800 nm, which primarily results from *cis*-$Ru(dcbpy)_2(NCS)_2$ cation absorption.[4] Appropriate monochromators and/or filters were used to minimize the probe light incident upon the sample. Transient data were collected with a silicon photodiode and digitized using a Tektronix TDS220 digital storage oscilloscope. The time resolution of the apparatus was ∼300 ns.

Potential control during the transient measurements was provided by a home-built potentiostat as described previously.[8] Such experiments were conducted either in the presence or absence of additional white light illumination (∼20 mW cm^{-2}, $\lambda > 475$ nm) generated by the 150 W tungsten lamp. The current drawn by the cell was monitored during all experiments.

Results

Current/Voltage Characteristics. Figure 2 exhibits the current−voltage curves of a typical dye sensitized solar cell employing the Epichlomer-16/NaI/I_2 polymer electrolyte measured at light intensities between 1 and 100 mW cm^{-2}. The optimum performance is obtained when the cell is irradiated at 10 mW cm^{-2}, yielding a fill factor (FF) of 73%, a short circuit current density J_{sc} of 0.5 mA cm^{-2}, an open-circuit voltage V_{oc} of 0.74 V and an overall efficiency (η), of 2.6%. At an irradiance of 100 mW cm^{-2}, which approximates to the standard AM1.5 irradiance, the values of J_{sc} and V_{oc} are increased to 4.2 mA cm^{-2} and 0.82 V respectively, FF is markedly reduced to 47% and η is reduced to 1.6%. Such J_{sc} values are approximately 50% of those obtained for comparable liquid junction devices employing a $LiClO_4/I_2$/*tert*-butylpyridine/acetonitrile electrolyte.[19] The high value for V_{oc} is particularly noteworthy, being in excess of that typically achieved for comparable liquid electrolyte devices.

These current−voltage curves can be fit to a two diode model of the form

$$I = I_L - I_0\left(\exp\left(\frac{qV_j}{m_1 k_B T}\right) - 1\right) - kI_L\left(\exp\left(\frac{qV_j}{m_2 k_B T}\right) - 1\right) \quad (1)$$

where I_L is the light intensity dependent short circuit current, k_B is Boltzmann's constant, T is temperature and I_0, k, m_1 and m_2 are fitting constants. Fits to the data using eq 1 are shown in Figure 2a (dashed lines). The bias dropped across the internal junction, V_j can be related to the externally applied bias, V, through

$$V_j = V + IR_S \quad (2)$$

where R_S is the series resistance of the system.

The first two terms on the right of eq 1 represent a voltage independent photocurrent, I_L, and a light independent recombination or "dark" current, and together compose the usual nonideal one diode current voltage characteristic for a photovoltaic cell.[26] In our system, the dark current corresponds to recombination reaction k_{cr2} in Figure 1. The final term in eq 1 is a *light dependent* recombination current, and is required to describe adequately the observed behavior for the polymer electrolyte cells. The choice of the form of this term is empirical but follows from the observations that the additional recombination current increases with light intensity, and hence with short circuit photocurrent, and that the net recombination current is exponentially increasing, as would be expected from the increasing occupation of electron acceptor states as the Fermi level is raised. The physical origin of this light intensity dependent recombination pathway will be discussed in detail below.

A good fit is obtained for the complete data set by fitting the data to eq 1 with the following parameter values: $R_S = 60 \pm 2\ \Omega$, $m_1 = 2.36 \pm 0.1$; $I_0 = 1.3 \pm 0.03$ nA; $m_2 = 4.04 \pm 0.4$; $k = (1.9 \pm 0.1) \times 10^{-4}$. The values for R_S, m_1, and I_0 were determined first by fitting the dark I−V data, and the values for m_2 and k by fitting the I−V curves at different light intensities. The high series resistance is consistent with the low ionic conductivity of the polymer electrolyte (∼10^{-5} S cm^{-1}). Fits obtained with these parameters are shown in Figure 2a.

It was also attempted to fit the data with the simple one-diode model (i.e., by setting $k = 0$ in eq 1). This simplified model was found to give reasonable fits to light intensity dependence of current /voltage curves of analogous dye sensitized solar cells employing liquid electrolytes (data not shown), in agreement with previous studies.[21] However, as illustrated in Figure 2b, the simplified model was unable to fit the light intensity dependence of current /voltage curves for light levels > 10 mW cm^{-2}. The disagreement does not result from series resistance effects, which are already included, nor does

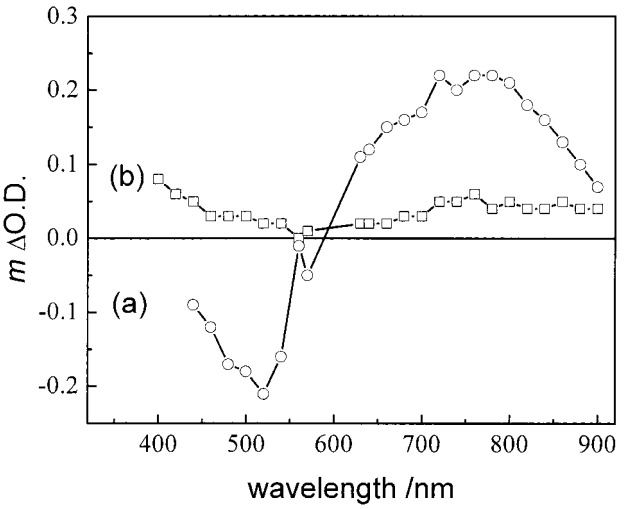

Figure 3. Transient absorption difference spectra obtained for TiO_2/$Ru(dcbpy)_2(NCS)_2$ /polymer electrolyte films 10 μs (curve a) and 1 ms (curve b) after optical excitation at 600 nm. The polymer electrolyte comprised of Epichlomer-16 with 9% NaI (w/w).

it appear to result from a voltage dependent photocurrent—a common phenomenon in other thin film PV materials such as amorphous silicon—because the currents reported here remain constant well into forward bias.

Transient Absorption Data for TiO_2/Dye/Polymer Electrolyte Films. Figure 3 shows the transient absorption difference spectra obtained for a dye sensitized TiO_2 films covered in Epichlomer-16/NaI polymer electrolyte at 10 μs (curve a) and 1 ms (curve b) after laser excitation at 600 nm. The spectrum obtained at 10 μs (curve a, Figure 3) is characteristic of the dye cation state formed by electron injection into the TiO_2 electrode.[4] It exhibits a negative feature between 450 and 580 nm assigned to the bleaching of the dye ground-state absorption, and a positive feature above 600 nm assigned to an LMCT transition of the cation state.[28] Electrons injected into the titania are also expected to give rise to a positive absorption increase in the red/near-infrared.[29] This absorption is, however, weak relative to the dye cation absorption and could not be observed directly in our experiments. The transient spectrum obtained for the same sample at 1 ms (curve b, Figure 3) exhibits two positive features from 420 to 550 nm and above 650 nm. Comparison with a previous pulse radiolysis study indicates that this spectrum is consistent with the I_2^- radical.[30] Again absorption from injected electrons is also likely to contribute to this spectrum, but appears to be weak relative to the I_2^- radical absorption. We attribute the I_2^- radicals observed in Figure 3 (curve b) to the rereduction of the dye cation by iodide ions, k_{rr}, according to

$$D^+ + 2I^- \rightarrow D + I_2^- \qquad (3)$$

An alternative route, based on the reduction of I_2 or I_3^- species by photoinjected electrons into the TiO_2, can be ruled out as the data shown in Figure 3 were collected without any addition of iodine to the electrolyte. Furthermore, the yield of I_2^- was found to be insensitive to the presence of iodine in the polymer electrolyte (see below). We note that the detailed reaction pathway for the regeneration reaction is at present unclear. However, previous studies have supported the formation of I_2^- as a product of reaction between the dye cation and the iodide ions. We note moreover that iodide oxidation to I_2^- radical is more thermodynamically favorable than the reaction leading to iodine formation.[31] A more complete analysis of these assignments, based upon our parallel studies of the dye cation regeneration reaction in liquid electrolytes, will be presented elsewhere.[32]

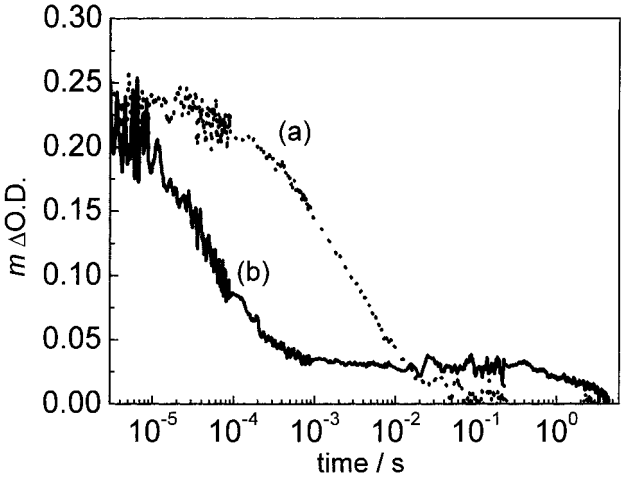

Figure 4. Transient absorption kinetics observed for TiO_2/$Ru(dcbpy)_2(NCS)_2$ /polymer electrolyte films at a probe wavelength of 800 nm. The polymer electrolyte comprised Epichlomer-16 with 9% $NaClO_4$ ((a): dotted line) and 9% NaI ((b): solid line). The data are highly nonexponential and for this reason plotted on a logarithmic time axis. In the absence of iodide ions in the polymer electrolyte (curve (a)), the decay is assigned to charge recombination between electrons in the TiO_2 and dye cations (k_{cr1}). In the presence of iodide ions (curve (b)), two phases to the decay are observed. The fast phase (microseconds) is assigned to dye cation decay due to k_{rr} (and k_{cr1}), with the concomitant generation of I_2^- radicals, whereas the slow phase (milliseconds) is assigned to decay of these I_2^-.

Figure 4 shows the transient absorption kinetics observed at 800 nm for dye sensitized TiO_2 films in the presence of a nonredox active polymer electrolyte (Epichlomer-16 + 9% $NaClO_4$ (w/w)), curve a, and in the presence of iodide containing polymer (Epichlomer-16 + 9% NaI (w/w)), curve b. In both cases, decay of the induced absorption signal, is not monoexponential.[8] In the absence of any redox active electrolyte, curve a, the cation excited state is rereduced by charge recombination with electrons occupying conduction band/trap states of the TiO_2 (k_{cr1}).[8] Monitoring the decay kinetics of this photoinduced absorption is, therefore, a probe of this charge recombination. This process is relatively slow and can be roughly quantified by the time needed to reach half of the initial absorbance,$\tau_{1/2}$, equal to 2 ms. This charge recombination half time is similar to that we have reported previously for dye sensitized TiO_2 films in nonredox active liquid electrolytes in the absence of external applied bias.[8,9] Recently, Haque et al, reported that the kinetics of this charge recombination are strongly dependent upon external applied bias, electrolyte composition and light intensity.[9] On the basis of these experimental data, Nelson has proposed a model to fit this reaction, being controlled by electron transport between an energetic distribution of trap sites within the TiO_2 nanoparticles.[33]

In the presence of I^- ions (Figure 4, curve b), the decay of the photoinduced absorption at 800 nm is biphasic. Following the assignments of the spectra shown in Figure 3, the fast phase ($\tau_{1/2-50}$ μs) is assigned to decay of the dye cation, whereas the slow phase is assigned to decay of I_2^- radicals generated by eq 1. The initial yield of dye cations, determined from the initial amplitude of the signal, is independent of the composition of the polymer electrolyte, consistent with a high yield of electron injection into the TiO_2 electrode. Decay of the dye cation may result from both rereduction by iodide ions, k_{rr}, and charge recombination with injected electrons k_{cr1}. The observation of

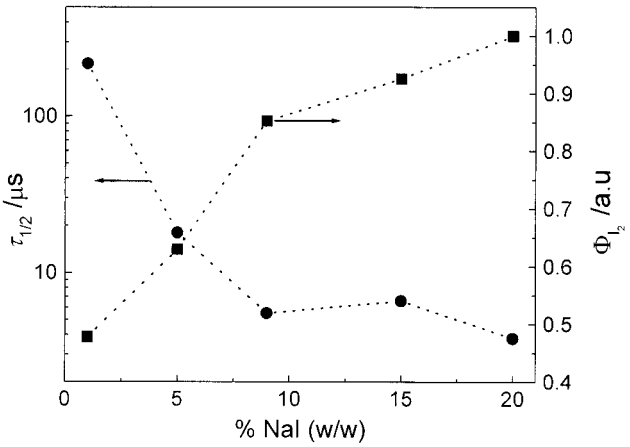

Figure 5. Plots of $\tau_{1/2}$ and I_2^-yield vs iodide concentration for the dye-sensitized TiO_2 film covered with the polymer electrolyte determined from absorption transients such as those shown in Figure 4. $\tau_{1/2}$ was defined as the half time of the fast decay phase apparent in Figure 4, curve (b), and the relative I_2^- yield was determined from the magnitude of the slow phase also apparent in this curve. The NaI concentration in the polymer ranged from 1 to 20% (w/w) (with the Na^+ concentration being kept constant by the co-addition of $NaClO_4$). Other experimental conditions were as for Figure 4.

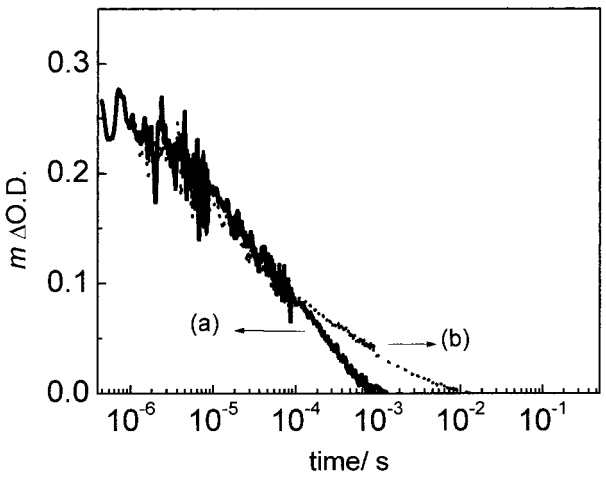

Figure 6. Transient absorption decays observed at 800 nm for complete photovoltaic cells under white light illumination and under applied bias. Samples were identical to those employed in Figure 3, except for the co-addition of iodine to the polymer electrolyte, and the addition of a platinised counter electrode. Data were collected under approximately 20 mW cm^{-2} white light illumination at short circuit ((a): solid line) and open circuit, $V_{oc} = 0.75$ V ((b): dotted line).

a significant yield of I_2^- radicals strongly indicates that the former occurs with a high yield. This conclusion is furthermore consistent with the significant acceleration of the dye cation decay observed in the presence of iodide ions (from 2 ms to 50 μs).

We addressed further the kinetic competition between k_{cr1} and k_{rr} by determining the transient kinetics at 800 nm as a function of concentration of iodide in the polymer electrolyte. The concentration of NaI was varied between 1 and 20%, with the concentration of Na^+ being kept constant by the co-addition of $NaClO_4$. Figure 5 shows plots of the dye cation decay time, $\tau_{1/2}$, and relative I_2^- yield, $\Phi_{I_2^-}$, as a function of iodide concentration. It is apparent that both the dye cation decay time and I_2^- yield are strongly dependent upon iodide concentration up to 9% NaI (w/w). This concentration dependence appears to saturate for concentrations >9%.

The observation that both $\tau_{1/2}$, and $\Phi_{I_2^-}$ are dependent upon iodide concentrations ≤9% NaI (w/w) is clearly indicative of kinetic competition between the charge recombination reaction, k_{cr1}, and the dye regeneration reaction, k_{rr}. As the concentration of I^- is increased, the rate of the regeneration reaction k_{rr} is expected to increase, resulting in an acceleration of dye cation decay kinetics and an increase in the yield of the I_2^- product states of this reaction. The saturation in this behavior for concentrations >9% NaI (w/w) is consistent with our previous ionic conductivity measurements of the polymer electrolyte,[24] which found that the film with 9% NaI (w/w) presented the highest ionic conductivity. Above this concentration, a 10-fold decay in the ionic conductivity was observed and attributed to a decrease of polymer chain mobility induced by the increase of the salt content. We note that a more quantitative analysis of the kinetic competition between k_{cr1} and k_{rr} is complicated by the nonexponential nature of the kinetics, as we discuss in detail elsewhere.[32] At 9% NaI, as employed for the I/V analyses shown in Figure 2, the yield of I_2^- product states is ~0.7 of the saturating value, in reasonable agreement with our observed photocurrent quantum efficiencies.[20]

Comparison of Figures 4 and 5 also indicate that the dye cation decay depends on not only iodide concentration but also Na^+ concentration. The half time for the dye cation decay, $\tau_{1/2}$ varies from 50 μs for the polymer electrolyte in the presence of $[Na^+] = 9\%$ (curve b, Figure 4) to 6 μs for the polymer electrolyte filled with $[Na^+] = 20\%$ (Figure 5). In both data, $[I^-]$ was constant and equal to 9%. Recently, Pelet et al suggested that dye cation rereduction rate by iodide ions depends strongly on the nature and concentration of "potential determining" cations.[31] This acceleration in the kinetics of D^+ state reduction can be assigned to the positive charge induced by the Na^+ ions absorbed into TiO_2 surface causing I^- to efficiently adsorb onto the oxide, leading to a faster I_2^- formation.

The results presented in Figure 5 are indicative that kinetic competition between charge recombination and dye regeneration by the electrolyte may limit the output current of the cell. In previous studies employing redox inactive liquid electrolytes, we have shown that the charge recombination dynamics are strongly dependent upon the Fermi level of the TiO_2 film.[8,9] If this was also the case for the polymer electrolyte cells studied here, this might be expected to result in the kinetic competition between k_{rr} and k_{cr1} also being dependent upon TiO_2 Fermi level, and therefore cell voltage. To address this issue, transient absorption data were collected under white light illumination for complete dye sensitized photoelectrochemical cells employing polymer electrolyte. Devices were identical to the dye sensitized TiO_2/polymer electrolyte films studied above except for the addition of 0.9% I_2 (w/w) and the use of a platinised counter electrode. Control data collected in the dark under open circuit conditions determined that neither the addition of iodine nor platinised counter electrode affected the dye cation decay kinetics, although they did result in reduction in the I_2^- lifetime, preventing its decay being temporally resolved from the dye cation decay at 800 nm.

Figure 6 shows absorption transients recorded at 800 nm of devices under white light illumination at short circuit ($I_{sc} = 0.6$ mA cm^{-2}) (curve a) and open circuit (curve b) V_{oc}, ca. 0.75 V. It is apparent that the half time for the decays at short circuit and open circuit are indistinguishable within experimental error ($\tau_{1/2} = 46$ and 48 μs respectively). The difference between the two traces at long times most probably arises from residual contributions to the data from I_2^- species. These half times are moreover similar to those observed in the absence of white light illumination (e.g Figure 4, trace (b), ($\tau_{1/2} = 50$ μs). We thus

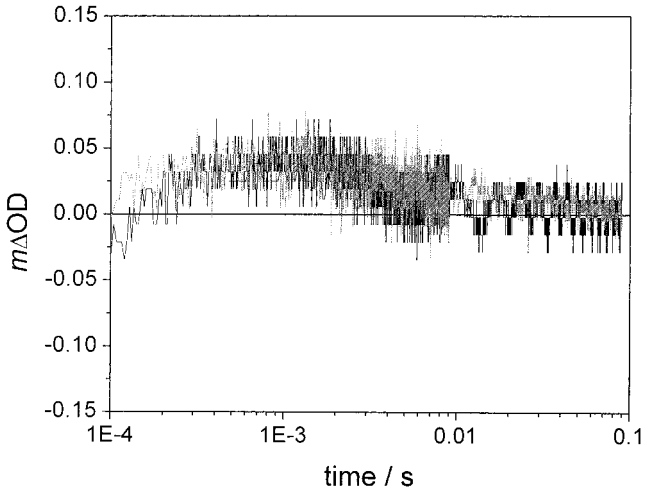

Figure 7. Transient absorption data collected as for Figure 6, but employing a probe wavelength of 500 nm. Data shown at short circuit ($V = 0$ gray line)and open circuit ($V = V_{oc} \sim 0.75$ V black line).

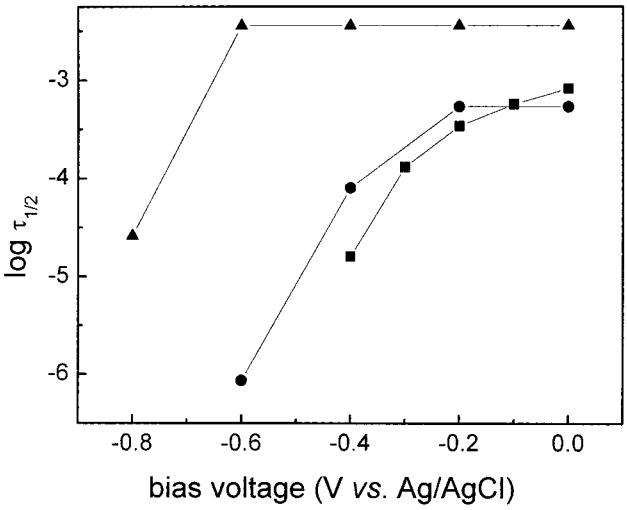

Figure 8. Plot of log $\tau_{1/2}$ vs applied potential to the dye sensitized TiO_2 electrode in a three electrode electrochemical cell, employing different electrolytes in propylene carbonate: (-■-) 0.1 M $LiClO_4$; (-●-) 0.1 M $NaClO_4$; (-▲-) 0.1 M $NaClO_4$ with additional 0.5 M *tert*-butyl-pyridine. As for Figure 5, $\tau_{1/2}$ refers to the half time for decay of the dye cation absorption, monitored at 800 nm, this decay is assigned to the recombination reaction k_{cr1}, following procedures detailed in full in ref 6. Potentials are given relative to an Ag/AgCl reference electrode.

conclude that the dye cation decay kinetics are essentially independent of either illumination or cell voltage.

We further note that the initial magnitudes of the transient signals in Figure 6 are also independent of cell voltage, indicating that yield of dye cations generated by electron injection is also independent of illumination or cell voltage. This is consistent with our recent studies of the electron injection kinetics as a function of TiO_2 Fermi level.[34]

The observation that the dye cation yield and decay kinetics are essentially independent of cell voltage suggests the yield of I_2^- radicals should also be invariant. To address this issue, further data were collected at a probe wavelength of 500 nm. At this wavelength, dye cations and I_2^- radicals generate absorption changes of opposite sign (see Figure 3) and can therefore be more readily distinguished (this wavelength has however the disadvantage that probe light is strongly absorbed by the sample, and therefore control "dark" data cannot be collected). Figure 7 shows such data employing a 500 nm probe wavelength for the photoelectrochemical cell under white light illumination at short and open circuit. In both cases, a positive signal is observed for time delays >c 200 μs, assigned to I_2^- formation. The magnitude of this positive signal is independent of cell voltage. We thus conclude that the yield of of I_2^- is independent of cell voltage, consistent with the observation made in Figure 6 that the dye cation decay kinetics are also independent of cell voltage.

The observation that the dye cation decay kinetics and I_2^- yield are independent of cell voltage up to 0.75 V suggest that at least over this voltage neither k_{rr} nor k_{cr1} are strongly dependent upon cell voltage. The voltage independence of k_{rr} is discussed in detail elsewhere.[32] The apparent voltage independence of k_{cr1} is however more surprising; we have shown previously for a range of different electrolytes that the recombination reaction can be strongly dependent upon applied voltage.[9] To address this issue further, we determined the voltage dependence of the charge recombination kinetics, k_{cr1}, in the absence of iodide ions by employing a three-electrode photoelectrochemical cell and a range of redox inactive liquid electrolytes. These studies employed propylene carbonate, as we show elsewhere the high viscosity of this solvent results in iodide rereduction kinetics readily comparable to those reported here for the polymer electrolyte. Experiments were conducted for propylene carbonate electrolytes containing 0.1 M $LiClO_4$, 0.1 M $NaClO_4$ and 0.1 M $NaClO_4$ with the addition of 0.5 M *tert*-butyl-pyridine. This base, *tert*-butyl-pyridine, was added to investigate the effect of the Lewis base character of the ethoxide groups of the Epichlomer-16 polymer, whereas a lithium salt was studied as lithium rather than sodium cations are routinely employed in liquid electrolyte photoelectrochemical cells. Lithium salts were not employed in the polymer electrolyte for the fabrication of dye sensitized solar cells as LiI was found to give a lower ionic conductivity in the polymer than NaI; this is assigned to the low dissociation constant of the LiI salt in the polymer matrix [Nogueira, A. F.; Paoli, M. de, unpublished results]. Figure 8 shows plots of $\tau_{1/2}$ for the recombination reaction k_{cr1} for these three different electrolytes as a function of voltage applied to the TiO_2 electrode relative to an Ag/AgCl reference electrode. Exchange of the electrolyte cation from lithium to sodium had only a marginal effect upon the recombination kinetics. However, it is apparent that the addition of *tert*-butyl-pyridine resulted in a significant retardation of the kinetics and shift of their voltage dependence to more negative potentials. In the presence of this base, the recombination dynamics were invariant in the range 0 to -0.6 V and only at -0.8 V is an acceleration of the charge recombination process observed, consistent with a study we have previously reported for acetonitrile/lithium based electrolytes.[9] Assuming a midpoint potential for the I^-/I_3^- redox couple of 0.2 V, this suggests that the charge recombination dynamics in dye sensitized photoelectrochemical cells employing such basic electrolytes would be independent of cell voltage up to 0.8 V, consistent with our transient studies of the polymer electrolyte cells at short circuit and open circuit detailed above. We thus suggest that the voltage independence of the dye cation decay kinetics observed for the polymer electrolyte device derives from the basic nature of the polymer employed.

Discussion

Studies of the function of dye sensitized photovoltaic cells to date have largely been based upon devices employing liquid electrolytes. We report here a study of the electron-transfer kinetics of a dye sensitized solar cell employing a polymer electrolyte based on an elastomer Epichlomer-16 containing NaI

and I_2. Such cells are particularly attractive due to their solid-state nature. In principle, such cells retain a volatile component, iodine. In practice, however, evaporation of iodine from the polymer electrolyte appears to be minimal, and the cells did not require any external sealing.

A key problem relating to the replacement of liquid by a polymer electrolyte is the lower ionic conductivity, typically achieved in these systems. The ionic transport in polymer electrolytes is coupled with polymer segmental motion. For ions to be transported through the polymer, the polymer chains must also move to promote formation of new coordination sites or free volume into which cations can migrate. It explains why the ionic transport in polymer electrolytes is confined to the amorphous phase in polymer−salt complexes. The particular polymer employed here has 16% of the epichlorohydrin units giving rise to a polymer with high ethylene oxide content but lower crystallinity than pure PEO. Thus, the addition of NaI results in a polymer electrolyte with reasonable ionic conductivity (1.5×10^{-5} S cm^{-1} at 30 °C, [H_2O] < 1 ppm).[24] However, this conductivity remains significantly lower than that achieved for liquid based electrolytes (e.g., $\sim 10^{-3}$ S cm^{-1} for liquid acetonitrile electrolytes).

The lower ionic conductivity of the polymer electrolyte has three primary implications for photovoltaic function:

(a) First, the lower conductivity increases voltage losses arising from charge transport through the electrolyte (i.e., the series resistance of the cell). Such losses are apparent in the current/voltage data shown in Figure 2, and are most important for high current densities. For this reason, technological applications of polymer electrolytes are likely to be limited to low power applications (e.g., indoor consumer products). At one sun illumination, our results indicate that this series resistance results in a voltage loss of up to 0.2 V between the internal junction and the external contacts, emphasizing the potential benefits of further improving polymer electrolyte conductivity.

(b) Second the lower ionic mobility is expected to retard the kinetics of dye cation reduction by iodide ions k_{rr}, as observed in Figure 4. The dye cation decay kinetics, attributed primarily to rereduction by I^-, exhibited a half time of 50 μs in the presence of the current polymer electrolyte, 2−3 orders of magnitude slower than the reduction kinetics observed in acetonitrile with a similar iodide concentration The slower rereduction kinetics obtained with the polymer electrolyte indicates that quantum yield losses associated with charge recombination, k_{cr1}, between electrons injected into the TiO_2 and photogenerated dye cations may be particularly important for these cells. Our studies as a function of iodide concentration in the polymer electrolyte suggest that this is indeed the case.

(c) Third the lower ionic conductivity can be expected to generate concentration gradients in the polymer electrolyte at high current densities. Importantly, the reduced mobility of I_3^- may lead to the buildup of triiodide in the pores relative to the bulk of the electrolyte, leading to increased probability of electron reaction with triiodide (k_{cr2}). Similarly, a relative depletion of iodide ions in the pores is expected, which may lead to a retardation of dye regeneration by the electrolyte (k_{rr}) and thus to an increased probability of electron−dye cation recombination, k_{cr1}. The additional, light dependent term required in eq 1 to fit the device current/voltage data is tentatively assigned to such loss pathways. This light dependent term is only required to fit current/voltage data for devices employing polymer electrolytes, but not for liquid electrolytes, consistent with the reduced ionic conductivity of the polymer electrolyte resulting in the generation of larger concentration gradients.

A particularly striking feature of the performance of the polymer electrolytes cells is their high open circuit voltage, 0.82 V. This is comparable or better than that obtained with liquid electrolyte cells, and significantly better than that achieved in previous studies of solid-state dye sensitized solar cells. This high V_{oc} can be in part attributed to the use in our cells of iodide/triiodide redox couple.[35] Previous studies of liquid electrolyte cells have indicated that recombination kinetics between injected electrons and triodide species are remarkably slow[36] consistent with the low dark currents observed for our cells (Figure 2).

Our previous studies of dye sensitized films in three electrode photoelectrochemical cells have indicated that the recombination reaction between injected electrons and photogenerated dye cations is strongly dependent upon electron density in conduction/trap states of the TiO_2 film, and therefore the Fermi level of the film. Given the relatively slow rereduction kinetics of the dye cation by iodide ions in the polymer electrolyte, this voltage dependence of k_{cr1} might be expected to be particularly critical for dye sensitized cells employing the polymer electrolyte. However, the data we show in Figures 6 and 7 indicate that this is not the case and suggest that at least up to a cell voltage of 0.75 V the recombination dynamics are independent of cell voltage, and therefore TiO_2 Fermi level. As we demonstrate in Figure 8, this observation can be attributed to the basic nature of the elastomer. This Figure demonstrates that, even in the presence of "potential determining" ions such as Li^+ or Na^+, the addition of a Lewis base to a liquid electrolyte results in a shift of the Fermi level dependence of the k_{cr} to more negative potentials. As we have shown previously, this shift results from a negative shift of the Fermi level dependence of electron occupancy of trap states of the TiO_2 film.[8,9] Several previous studies have observed a strong pH dependence of the conduction band/trap state energetics in nanocrystalline TiO_2 films, attributed to protonation/deprotonation of surface bound oxygen species.[29,37] Consideration of Figure 8 suggests that in the presence of added base (*tert*-butylpyridine), acceleration of the recombination kinetics to a $\tau_{1/2} < 1$ ms is only observed for applied voltages of < −0.6 V vs. Ag/AgCl, corresponding to a cell voltage (vs the iodide/triodide redox couple) of ~0.8 V.

It follows from the above that the Lewis base nature of the polymer, Epichlomer-16, is critical to the photovoltaic performance of the cell. We further note that this basic character, which will minimize the electron occupancy of TiO_2 trap states at a given cell voltage, is also likely to minimize dark current losses (k_{cr2}). We have also suggested elsewhere that the excellent penetration of the film pores by the polymer electrolyte, as demonstrated by data collected as a function of front/back illumination of the film, derives from acid/base interactions between the TiO_2 film and the polymer.[20] We conclude that the basic nature of poly(ethylene oxide) based polymers is particularly attractive for the application in dye sensitized photoelectrochemical solar cells as a solid-state electrolyte.

The studies we present here indicate a reasonable agreement between the electron-transfer kinetics and the photovoltaic device performance. A more quantitative analysis would require greater control of experimental conditions, in particular the position of the Fermi level of the TiO_2 film, and numerical modeling of the observed nonexponential decay kinetics. Such studies are presented elsewhere, in which we employ three

electrode photoelectrochemical cell and liquid electrolyte to achieve more direct control of the TiO_2 Fermi level.[32]

Acknowledgment. A.F.N. thanks FAPESP for a fellowship (Proc. Nr. 98/10567-6), the authors also thank financial support from FAPESP (Proc. Nr. 96/09983-6) and Daiso Co. Ltd, Japan for providing Epichlomer-16 samples. We would also like to thank Sven Södergren and Saif Haque for assistance with the conduction and analysis of the transient spectroscopic experiments and Richard Willis and Thierry Lutz for the fabrication of the TiO_2 particles. Financial support is also gratefully acknowledged from the EPSRC and Leverhulme Trust in the U.K. I.M. acknowledges the financial support of a Marie Curie Fellowship from the European Commission.

References and Notes

(1) O′Reagan, B.; Grätzel, M. *Nature* **1991**, *353*, 373.
(2) Nazeeruddin, M. K.; Kay, A.; Rodicio, I.; Humphrey-Baker, R.; Muller, E.; Liska, P.; Vlachopoulos, N.; Grätzel, M. *J. Am. Chem. Soc.* **1993**, *115*, 6382.
(3) Hagfeldt, A.; Grätzel, M. *Chem Rev.* **1995**, *95*, 49.
(4) Tachibana, Y.; Moser, J. E.; Grätzel, M.; Klug, D. R.; Durrant, J. R. *J. Phys. Chem.* **1996**, *100*, 20 056.
(5) Rehm, J. M.; McLendon, G. L.; Nagasawa, Y.; Yoshihara, K.; Moser, J.; Grätzel, M. *J. Phys. Chem.* **1996**, *100*, 9577.
(6) Asbury, J. B.; Ellingson, R.; J.; Ghosh, H. N.; Ferrere, S.; Nozik, A. J.; Lian, T. *J. Phys. Chem.* **1999**, *103*, 3110.
(7) Huber, R.; Spörlein, S.; Moser, J. E.; Grätzel, M.; Wachtveitl, J. *J. Phys. Chem. B* **2000**, *104*, 8995.
(8) Haque, S. A.; Tachibana, Y.; Klug, D. R.; Durrant, J. R. *J. Phys. Chem. B* **1998**, *102*, 1745.
(9) Haque, S. A.; Tachibana, Y.; Willis, R. L.; Moser, J. E.; Grätzel, M.; Klug, D. R.; Durrant, J. R. *J. Phys. Chem. B* **2000**, *104*, 538.
(10) Martini, I.; Hodak, J. H.; Hartland, G. V. *J. Phys. Chem. B* **1998**, *102*, 9508.
(11) Murakoshi, K.; Kogure. R.; Wada, Y.; Yanagida, S. *Sol. Energy Mater. Sol. Cells* **1998**, *55*, 113.
(12) Murakoshi, K.; Kogure, R.; Wada, Y.; Yanagida, S. *Chem. Lett.* **1997**, 471.
(13) Tennakone, K.; Kumara, G. R. R. A.; Wijayantha, K. G. U. *Semicond. Sci. Technol.* **1996**, *11*, 1737.
(14) O′ Reagan, B.; Schwartz, D. T. *J. Appl. Phys.* **1996**, *80*, 4749.
(15) Bach, U.; Lupo, D.; Comte, P.; Moser, J. E.; Weissortel, F.; Salbeck, J.; Spreitzer, H.; Gratzel, M. *Nature* **1998**, *395*, 583.
(16) Cao, F.; Oskam, G.; Searson, P. C. *J. Phys. Chem.* **1995**, *99*, 17 071.
(17) Matsumoto, M.; Miyasaki, H.; Matsuhiro, K.; Kumashiro, Y.; Takaoka, Y. *Solid State Ionics* **1996**, *89*, 263.
(18) Kubo, W.; Murakoshi, K.; Kitamura, T.; Wada, Y.; Habusa, K.; Shirai, H.; Yanagida, S. *Chem. Lett.* **1998**, *12*, 1241.
(19) Mikoshiba, S.; Sumino, H.; Yonetsu, M.; Hayase, S. *Proceedings in Thirtheenth International Conference on Photochemical Conversion and Storage of Solar Energy*, W6−70; Snowmass, USA, 2000.
(20) Nogueira, A. F.; Durrant, J. R.; De Paoli, M.-A. *Adv. Mater.* **2001**, in press.
(21) Bach, U.; Tachibana, Y.; Moser, J.-E.; Haque, S. A.; Durrant, J. R.; Grätzel, M.; Klug, D. *J. Am. Chem. Soc.* **1999**, *121*, 7445.
(22) Topoglidis, E.; Lutz, T.; Willis, R.; Barnett, C.; Cass, A. E. G.; Durrant, J. R. *Faraday Disc.* **2000**, *116*, 35.
(23) Barbé, C. J.; Arendse, F.; Comte, P.; Jirousek, M.; Lenzmann, F.; Shklover, V.; Grätzel, M. *J. Am. Ceram. Soc.* **1997**, *80*, 3157.
(24) Nogueira, A. F.; Spinacé, M. A. S.; Gazotti, W. A.; Girotto, E. M.; De Paoli, M.-A. *Solid State Ionics* **2001**, in press.
(25) The cell design in both cases being optimized for high optical transparency with nonscattering TiO2, nonreflective counter-electrode and high transmission 15 Ω/sq conducting glass.
(26) Sze, S. K. *Physics of Semiconductor Devices*, 2nd ed.; John Wiley & Sons Inc.: New York, 1981; 790.
(27) Södergren, S.; Hagfeldt, A.; Olsson, J.; Lindquist, S.-E. *J. Phys. Chem.* **1994**, *98*, 5552.
(28) Moser, J. E.; Noukakis, D.; Bach, U.; Tachibana, Y.; Klug, D. R.; Durrant, J. R.; Humphry-Baker, R.; Grätzel, M. *J. Phys. Chem. B* **1998**, *102*, 3649.
(29) Rothenberger, G.; Fitzmaurice, D.; Grätzel, M. *J. Phys. Chem.* **1992**, *96*, 5983.
(30) Devonshire, R.; Weiss, J. *J. Phys. Chem.* **1968**, *72*, 3815.
(31) Pelet, S.; Moser, J.-E.; Grätzel, M. *J. Phys. Chem. B* **2000**, *104*, 1791.
(32) Montanari, I.; Nelson, J.; Durrant, J. R., in preparation.
(33) Nelson, J. *Phys. Rev. B* **1999**, *59*, 15374.
(34) Tachibana, Y.; Haque, S. A.; Mercer, I. P.; Moser, J. E.; Klug D. R.; Durrant, J. R., submitted to *J. Phys. Chem.*
(35) Huang, S. Y.; Schlichthörl, G.; Nozik, A. J.; Grätzel, M.; Frank, A. J. *J. Phys. Chem. B* **1997**, *101*, 2576.
(36) Fisher, A. C.; Peter, L. M.; Ponomarev, E. A.; Walker, A. B.; Wijayantha, K. G. U. *J. Phys. Chem. B* **2000**, *104*, 949.
(37) Yan, S. G.; Prieskorn, J. S.; Kim, Y. J.; Hupp, J. T. *J. Phys. Chem. B* **2000**, *104*, 10 871.